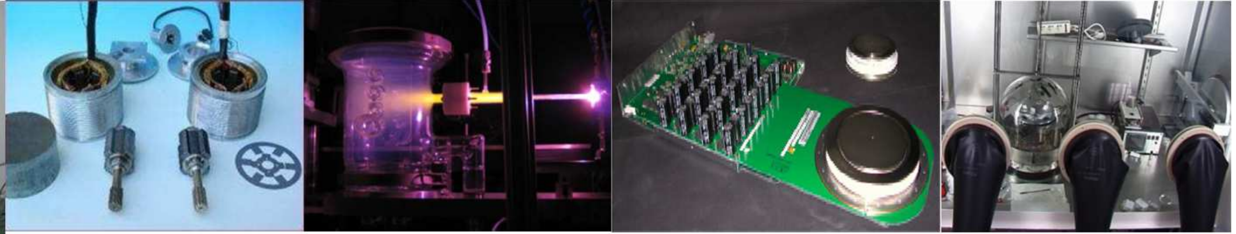
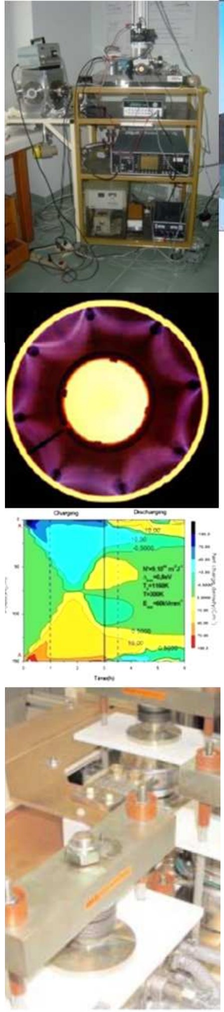

Laplace

Couplage PVD-PECVD pour le dépôt de couches minces nanocomposites à base de nanoparticules d'argent enterées dans une silice et applications

Kremena Makasheva

LAboratoire PLAsma et Conversion d'Energie (LAPLACE)

Université de Toulouse, CNRS, INPT, UPS, France

Université de Toulouse

Université Toulouse III Paul Sabatier

cnrs

INP ENSEEIHT

Journées d'Echanges du Réseau Plasmas Froids, Octobre 18th, 2016

Multifunctional thin dielectric layers containing AgNPs

A way for transition from material level of development to system level of applications

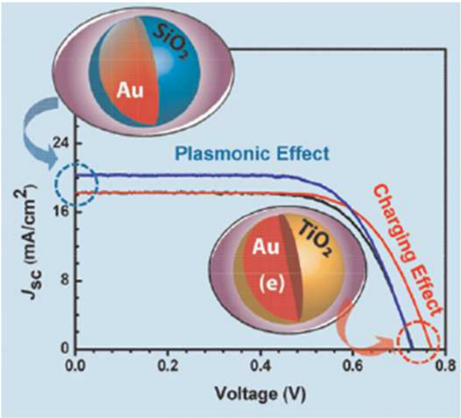

H. Choi et al., (2012) ASC Nano

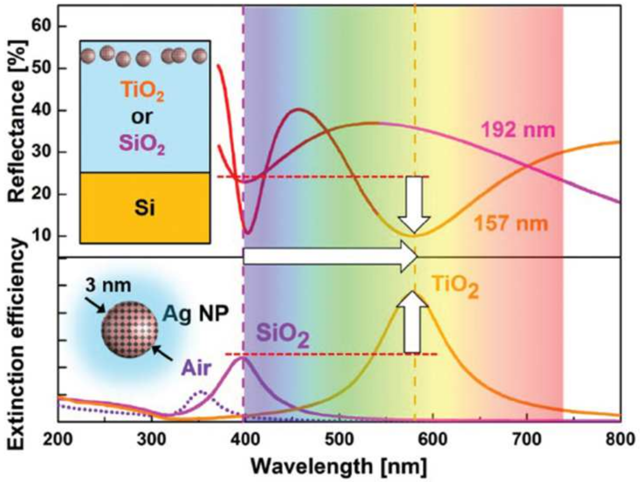

R. Carles et al., (2015) Nanoscale

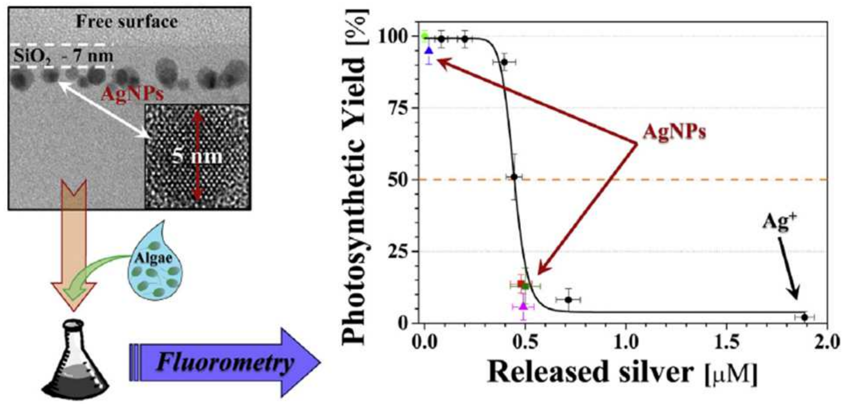

A. Pugliara et al., (2016) STOTEN

Optical, electrical, biocide properties

1. Advanced solar cells – combining plasmonic and charge trapping effects;
2. Control of charge injection in dielectrics – HVDC applications;
   – power electronics;
3. Plasmonic substrates – ultra-sensitive sensors for chemical and biological detection and analyses;
4. Biocide effect – modulation of toxicity level.

Outline

1. Plasmas as a versatile tool for deposition processes
2. RF asymmetric capacitively-coupled discharge
3. AgNPs as deep artificial traps of charges
4. AgNPs based plasmonic substrates
5. AgNPs for biological surface effects
6. Conclusions and perspectives

Non-Equilibrium Plasmas and types of gas discharges

Plasma is a medium composed of electrons and ions, free to move in all spatial direction.

M. Moisan, J. Pelletier (2012) *Physics of Collisional Plasmas*

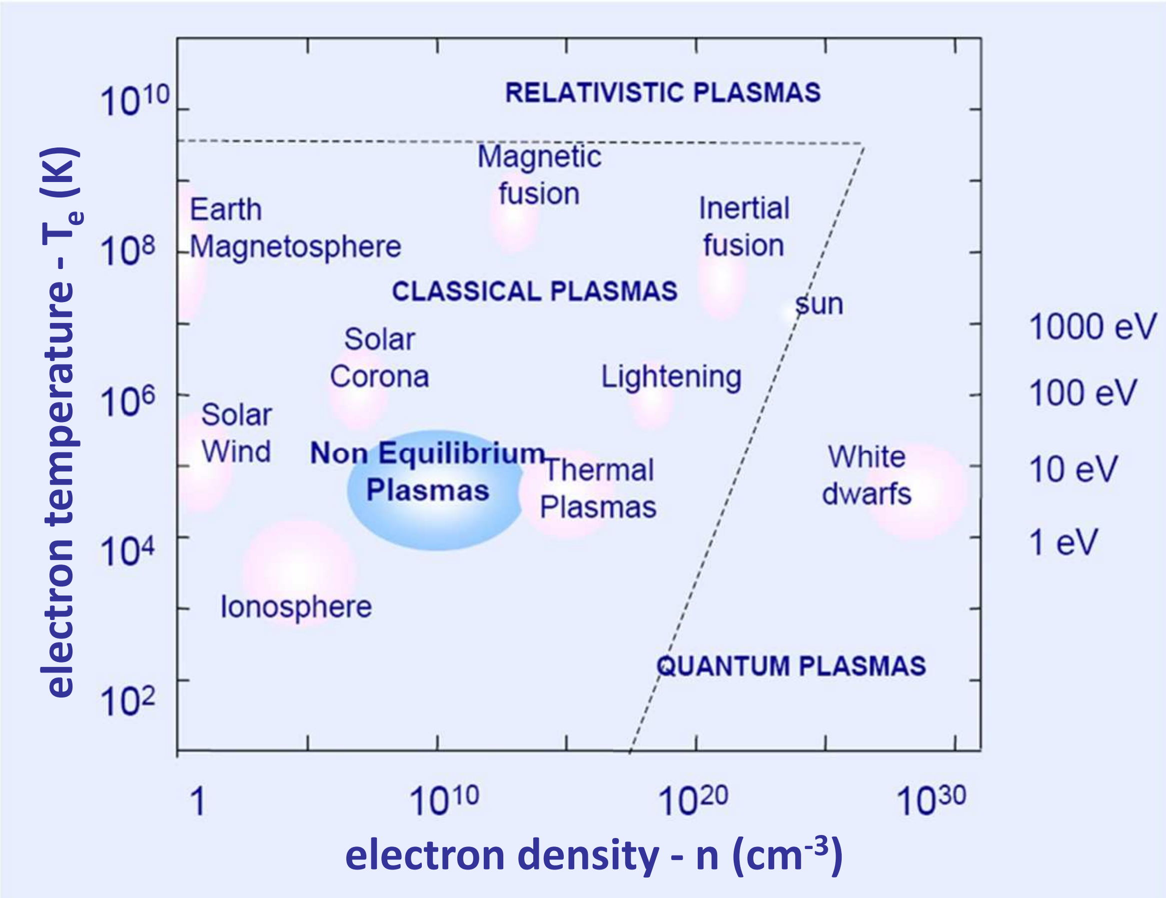

Non-equilibrium plasmas $T_e >> T_i; T_g$

$$\alpha_i = \frac{n_i}{n_i + N}$$ degree of ionization ($< 10^{-4}$)

The plasma is a macroscopically neutral medium

The plasma is a quasi-neutral medium

$$-\left(n_e e + n_{i\_} e\right) + \sum_z n_z Z e = 0$$

The maximum distance of non-neutrality is the Debye length

$$\lambda_D = \sqrt{\frac{\varepsilon_0 k_B T_e}{e^2 n_e}}$$

The plasma behaves as a collective medium

$$\omega_{pe} = \sqrt{\frac{e^2 n_e}{\varepsilon_0 m_e}}$$

Non-Equilibrium Plasmas and types of gas discharges

- Collisions (electrons ↔ neutrals) are needed for plasma generation (ionization)
- Energy ↔ plasma coupling is strongly dependent on the gas pressure
- Applications in a quite large range of gas pressures

Plasma ion sources, Propulsion, Magnetrons, ECR

Plasmas for microelectronics

Nanocomposites

Surface treatment

Lamps

Diamond synthesis

Plasma Display Panels, Microplasmas, Aerodynamic applications, Detoxification, Plasma for medicine

pressure: 0.1 — 1 — 10 — 10^2 — 10^3 — 10^4 — 10^5 Pa

$$p = N k_B T_g$$

$$\nu \propto N$$

mean free path - $\lambda_{f.p.}$: 1 m — 1 cm — 100 µm — 1 µm

$$\lambda_{f.p.} = \frac{v_{Th}}{\nu}$$

← magnetic → confinement

← DC, RF, microwave heating →

← DBD, microdischarges → microwave, pulsed discharges

Weakly ionized plasma; Gas pressure: 10 – 100 Pa; Power up to kW

=> Typical values of $T_e \cong$ 2-3 eV, $n_e \cong 10^9$ cm^{-3}

=> mean free path $\lambda_{f.p.} \cong$ 1 cm

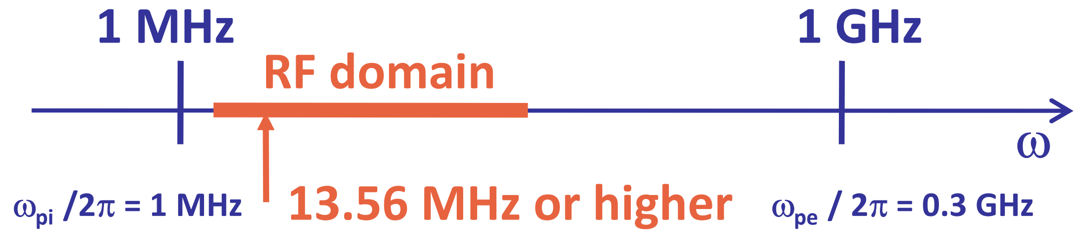

- **Electrons follow the rf field**
- **Ions follow time-averaged field**
- **Ohmic heating**
- **Collisionless power deposition**

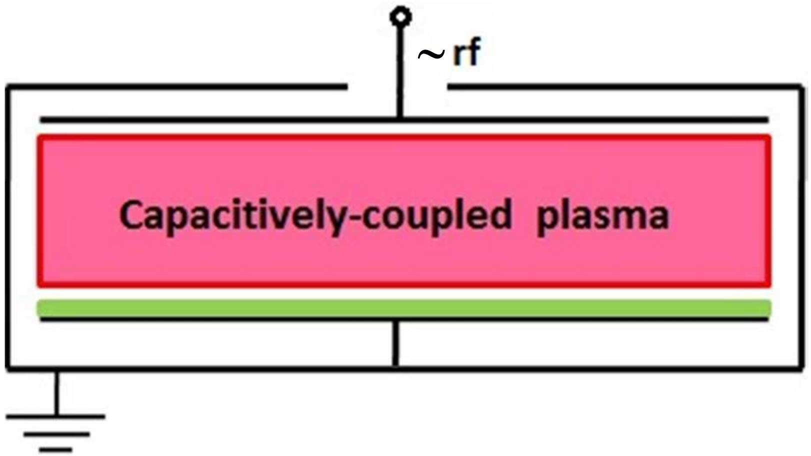

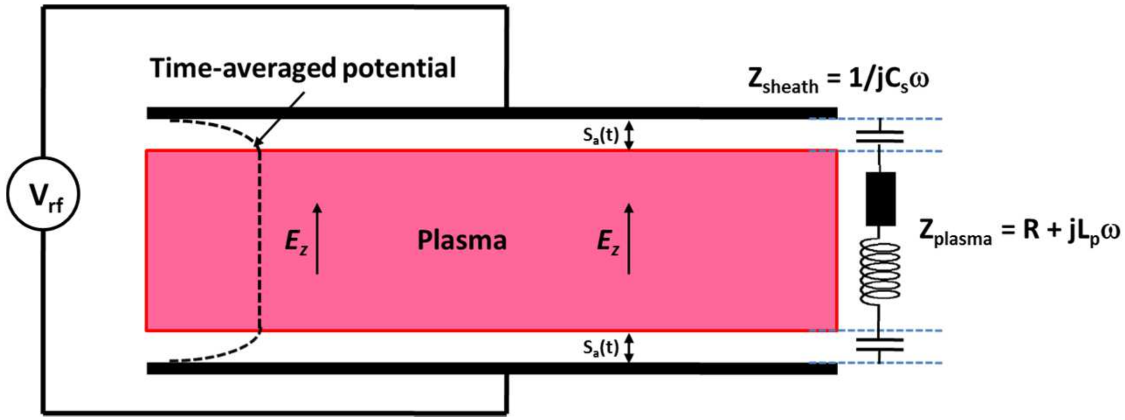

Plasma impedance depends on: - Voltage, V_{rf} ; Electron density, n_e; Sheath size, s_m

Yu. P. Raizer « Gas Discharges » Springer, Berlin, 1991.
M. A. Lieberman and A.J. Lichtenberg « Principles of Plasma Discharges and Material Processing » John Wiley & Sons, New York, 2005.
P. Chabert and N. Braithwaite « Physics of Radiofrequency Plasmas » Cambridge University Press, 2011.

Sputtering for thin layers deposition

1852 – Grove => deposition of thin metal layer on the discharge tube.
1877 – Wright => proposes the use of sputtering for deposition of thin metal layers.

1950 – Wehner => Momentum Theory

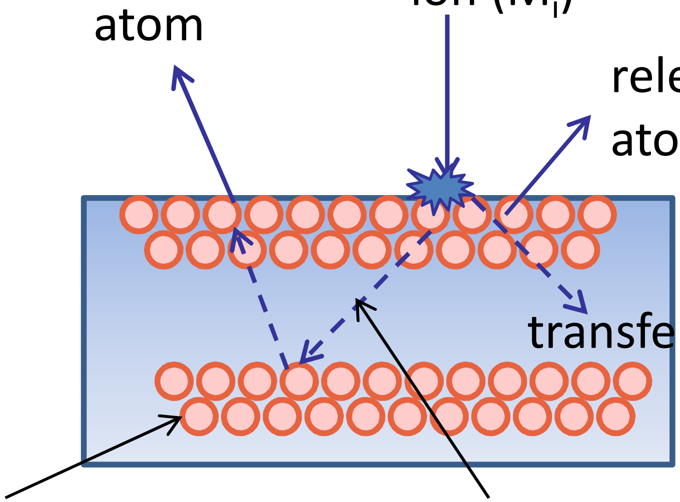

- **The sputtering rate depends on the ion mass and on the ion energy. It is very sensitive to the angle of incidence;**
- **It is a threshold process;**
- **The released atoms own higher energy compared to those from evaporation process;**
- **The sputtering rate decreases at very high energy due to implantation of incident ions;**
- **Secondary electron emission is low;**
- **Electrons do not add value to sputtering.**

$$S = \left(C_{ste}\right) \varepsilon \frac{E}{U} \alpha\left(M_t / M_i\right)$$

$$\varepsilon = \frac{4 M_i M_t}{\left(M_i + M_t\right)^2} E$$

A. Richardt and A.-M. Durand, « Vide » Edition IN FINE, Paris, 1995.

DC and RF magnetron sputtering, 0.1 Pa

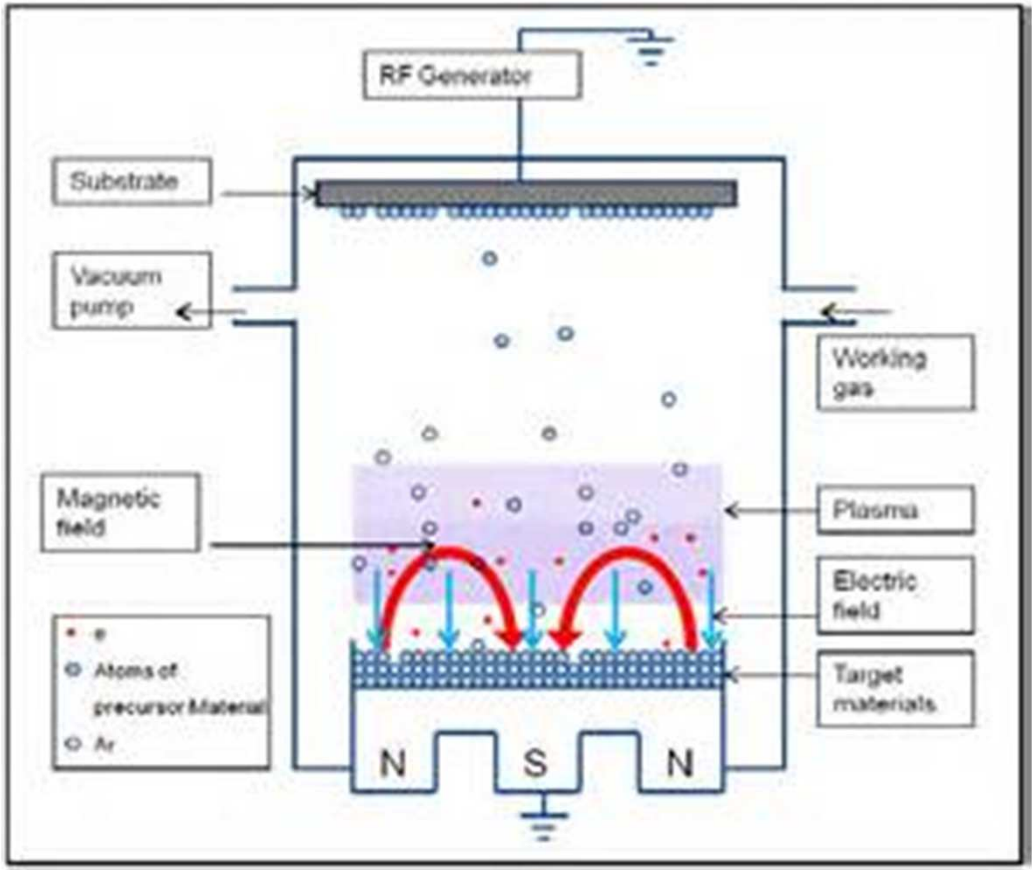

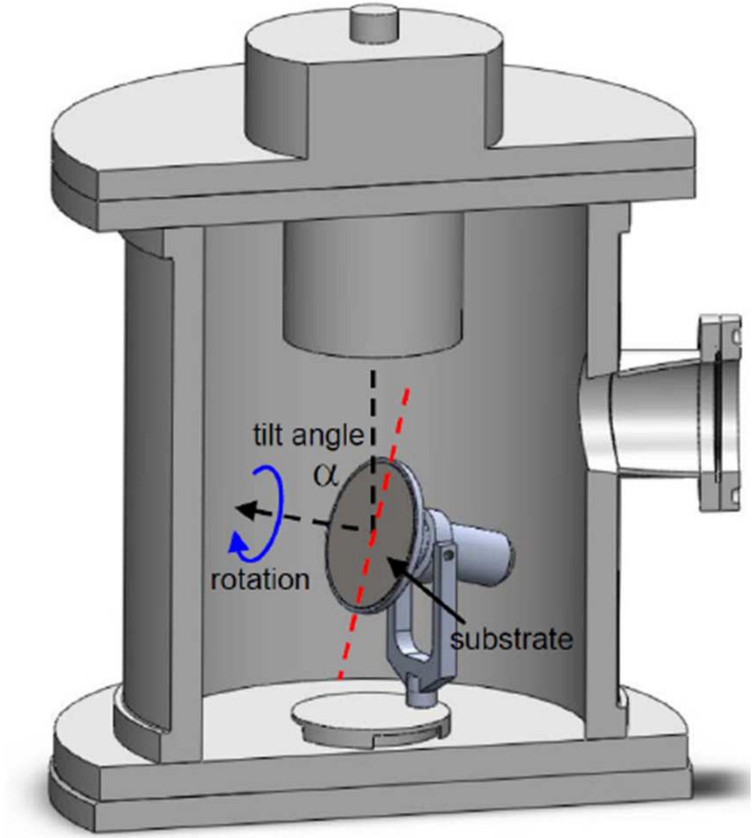

Réseau Plasmas Froids – Anne-Lise Thomann, GREMI, Orléans;
– Cécile Arnas, PIIM, Marseille;
– Jean-François Pierson, David Horvat, IJL, Nancy

RF asymmetric discharge

Deposition of nanocomposite materials containing Ag nanoparticles

☞ **Means** Radiofrequency asymmetric discharge sustained in Argon-Hexamethyldisiloxane mixture

☞ **Process** Silver sputtering and plasma polymerization of the Hexamethyldisiloxane

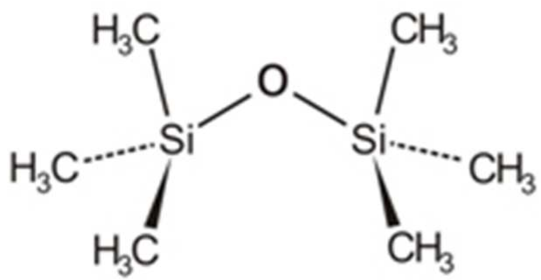

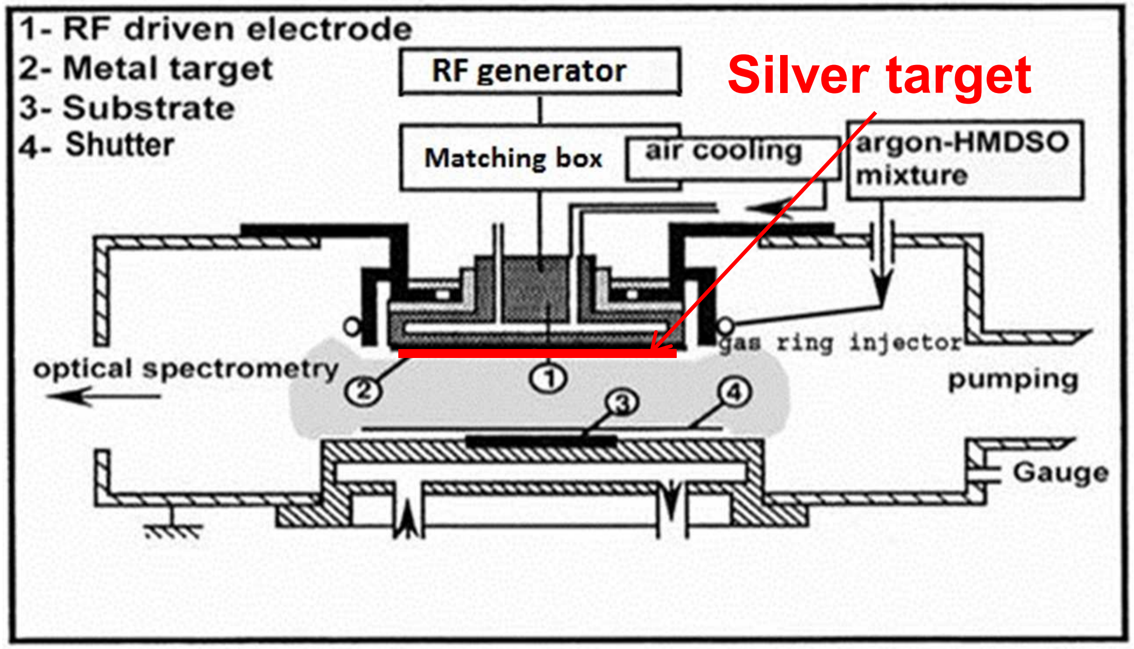

Chamber of metal- matrix deposition

☹ continuous injection of HMDSO leads to total covering of the silver target

☺ pulsed injection of HMDSO allows to control the composition of Ag/polymer matrix

E. Key and M. Hecq (1984) J. Appl. Phys. **55**, 370.
B. Despax et al., (2007) Plasma Process. Polym. **4**, 127.

Deposition procedure - simultaneous deposition

Step 1:
Simultaneously Ag sputtering and plasma polymerization
Ar + HMDSO discharge
(Ar + HMDSO + O_2)

P = 85 W; V_{dc} = - 791 V; p_{tot} = 43.8 mTorr;
HMDSO t_{on} = 1.6 s; T_{HMDSO} = 5 s
(Q_{HMDSO} = 0.144 sccm, p_{HMDSO} = 3.8 mTorr)
Deposition time: t_p = 10 min

AgNPs in SiOC:H

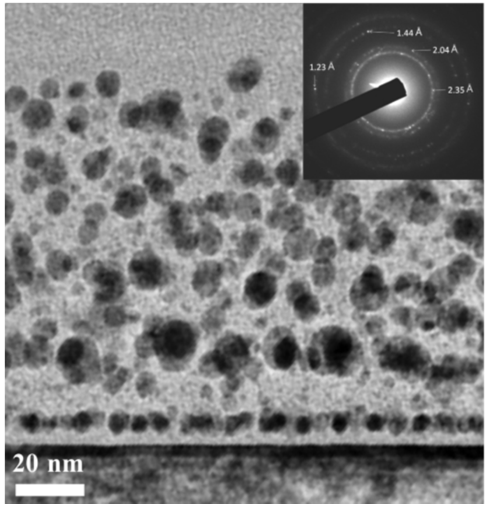

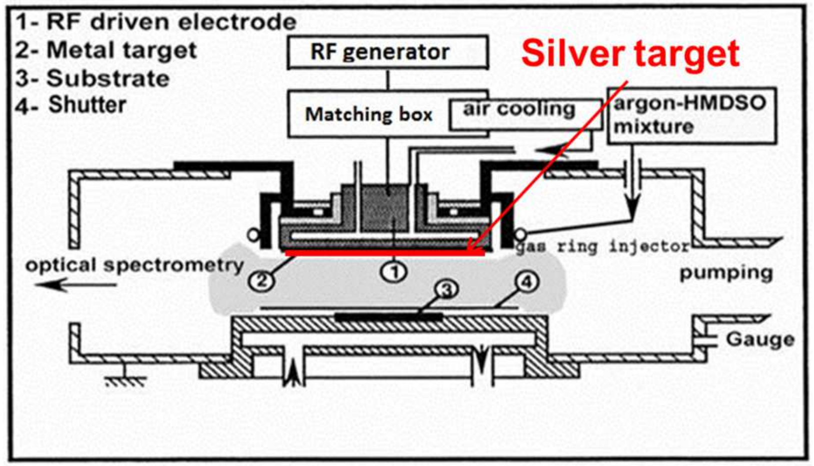

Chamber of metal- matrix deposition

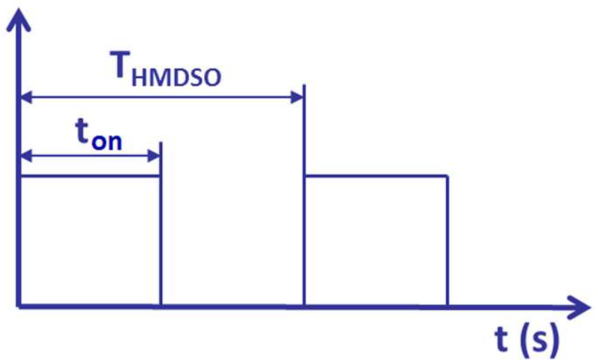

☺ **pulsed injection of HMDSO allows to control the composition of Ag/polymer matrix**

B. Despax et al., Plasma Process. Polym. 2007, **4**, 127.

Deposition procedure - simultaneous deposition

Plasma monitoring – Optical Emission Spectroscopy (OES)

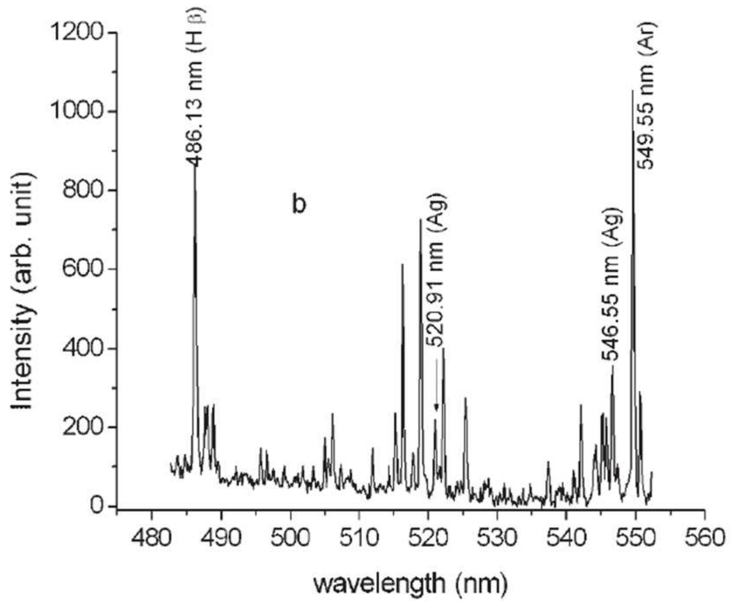

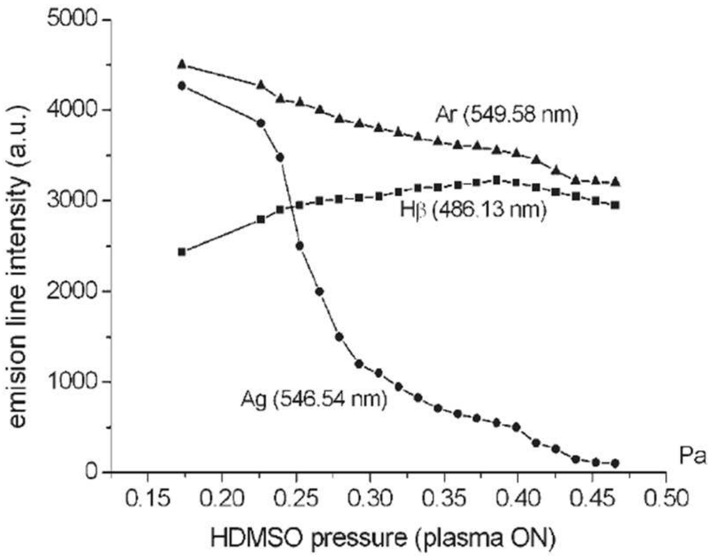

Rules for selection of optical lines for the line ratio:

- **Lines close to each other in wavelength**

$$\frac{I_{Ag(546.55nm)}}{I_{Ar(549.59nm)}} = \frac{\hbar \nu_{Ag}}{\hbar \nu_{Ar}} \frac{N_{Ag}}{N_{Ar}} \frac{A_{Ag}}{A_{Ar}} = \frac{g_{Ag}}{g_{Ar}} \frac{\nu_{Ag}}{\nu_{Ar}} \frac{A_{Ag}}{A_{Ar}} \exp\left(-\frac{U_{Ag} - U_{Ar}}{k_B T_e} \right)$$

close to unity

- **Intensive lines;**
- **Lines originating from hihgly excited levels, populated by direct excitation.**

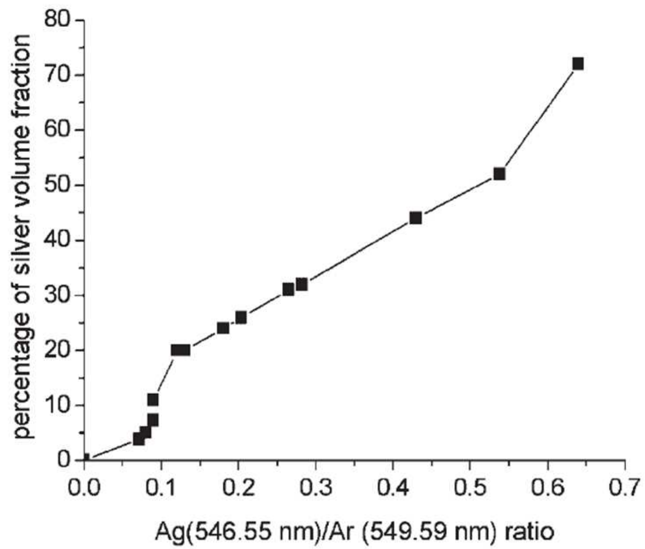

B. Despax et al., (2007) Plasma Process. Polym. **4**, 127.

Deposition procedure – successive deposition

Step 1:
Ag sputtering in Ar-discharge

$\overline{d} = 522.6 \pm 2.6 \text{ nm}$

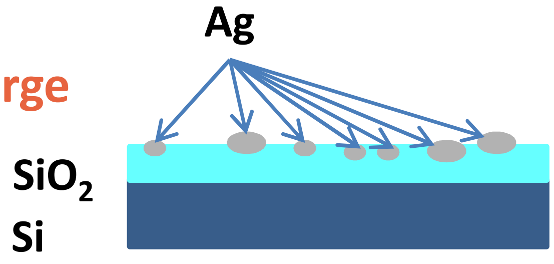

$P = 80$ W; $V_{dc} = -950$ V; $p_{Ar} = 40.8$ mTorr; $t_p = 5$ s

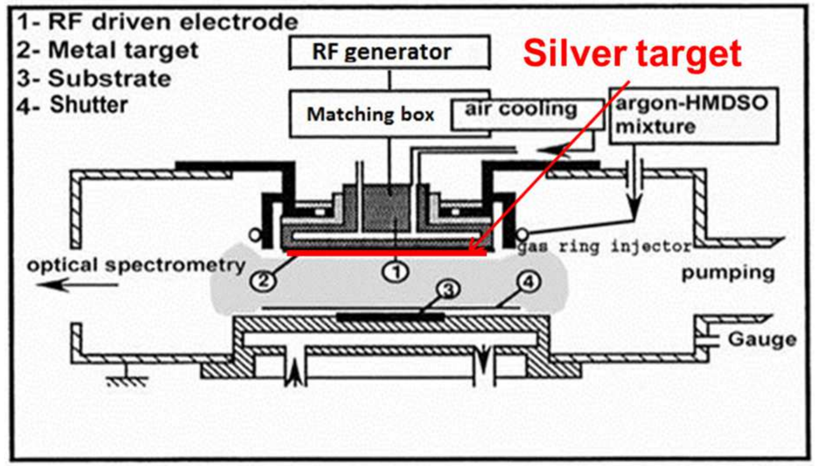

Chamber of metal- matrix deposition

Step 2:
Plasma polymerization
Ar + HMDSO discharge
(Ar + HMDSO + O_2)

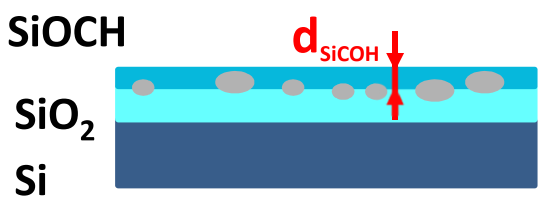

$Q_{HMDSO} = 0.4$ sccm, $P = 80$ W; $V_{dc} = -900$ V; $p_{tot} = 49.5$ mTorr

Deposition time:

$t_d =$ 30 s
$t_d =$ 3 min
$t_d =$ 10 min

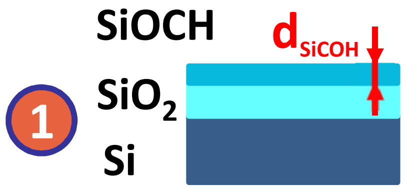

Thickness:
d_{11} = 545.8 nm
d_{12} = 598.5 nm
d_{13} = 757.0 nm

Thickness:
d_{21} = 24.2 nm
d_{22} = 75.3 nm
d_{23} = 221.2 nm

K. Makasheva et al. (2016) IEEE Trans. Nanotechnology

HVDC cables – advantages and drawbacks

European HVDC "SuperGrid" concept under the DESERTEC foundation proposal

DC SuperGrids represent just one third of the size of AC systems for the same load; pylons (where needed as many parts can be underground or undersea) are much smaller; DC stabilizes grids by allowing interconnection and rapid support for variations in capacity, much less losses than the transport under AC, stabilization of the network, easier interconnection, etc.

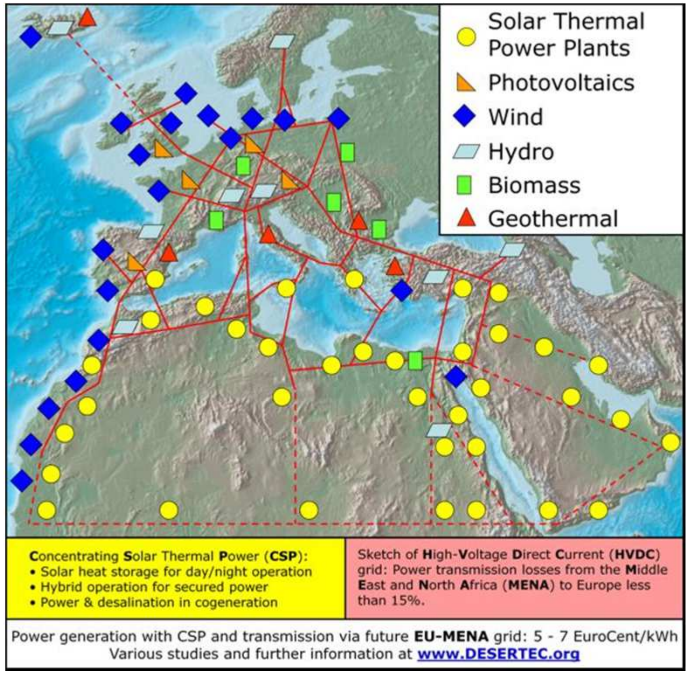

HVDC cables

In the HVDC cables with synthetic insulation the injected charges at the electrodes modify the local electric field distribution. It can provoke catastrophic issue during grounding phase of the connection or during polarity change of the line.

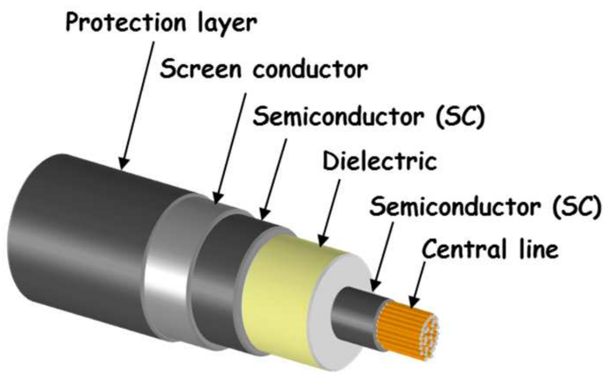

The main objective of this work is:
to control the formation of space charge in insulating synthetic materials for HVDC applications, focussing on polyethylene and its interfaces in HVDC systems.

Collaboration -> C. Laurent and G. Teyssedre, Solid Dielectrics and Reliability - DSF group, LAPLACE

AgNPs as deep artificial traps of charges

Strategy to limit the charge injection and charge transport

Introduction of deep artificial traps of charges at the interface electrode/insulation through a single layer of silver nanoparticles with controlled size and density

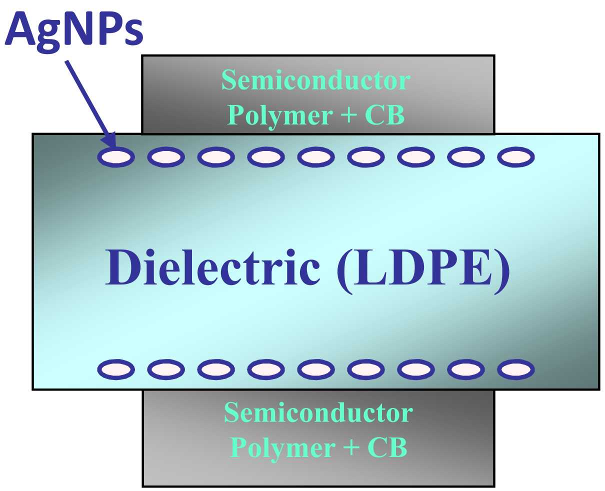

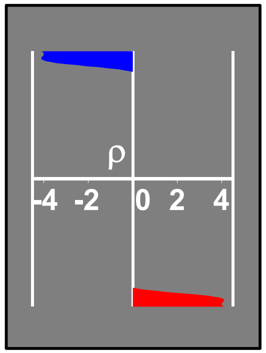

Density of electric charges needed to compensate an electric field of 2×10^7 V/m:

$$\Delta E = \frac{\rho_s}{\varepsilon}$$

$$n_s = \frac{\Delta E\, \varepsilon}{e} = 2 \times 10^{11}\ \text{cm}^{-2}\ \left(d \approx 20\ \text{nm}\right)$$

Deposition procedure – successive deposition

RF asymmetric discharge

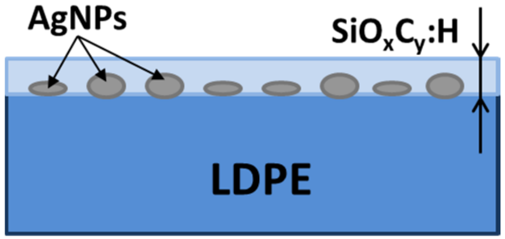

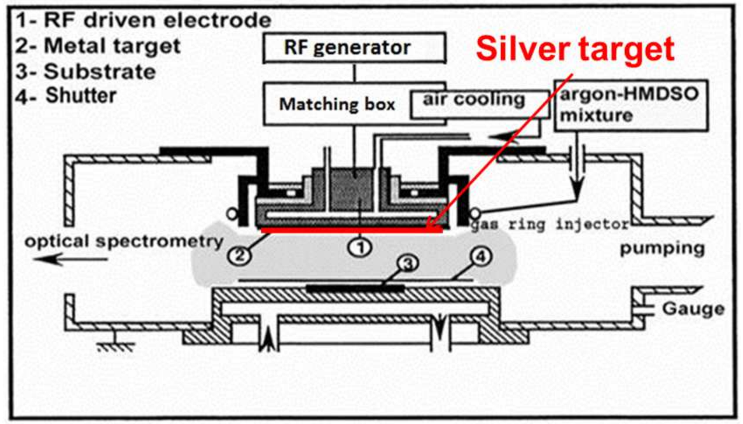

Chamber of metal- matrix deposition

Step 1:
Ag sputtering in Ar-discharge

p_{Ar} = 5.32 Pa,
P = 80 W, V_{dc} = - 950 V, t_s = 5 s

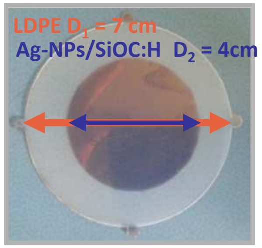

Step 2:
Plasma polymerization
Ar + HMDSO discharge

p_{tot} = 6.6 Pa, Q_{HMDSO} = 0.4 sccm,
P = 80 W, V_{dc} = - 900 V, t_d = 60 s

L. Milliere et al., (2014) APL, **105**, 122908.

Optical emission spectroscopy (OES)

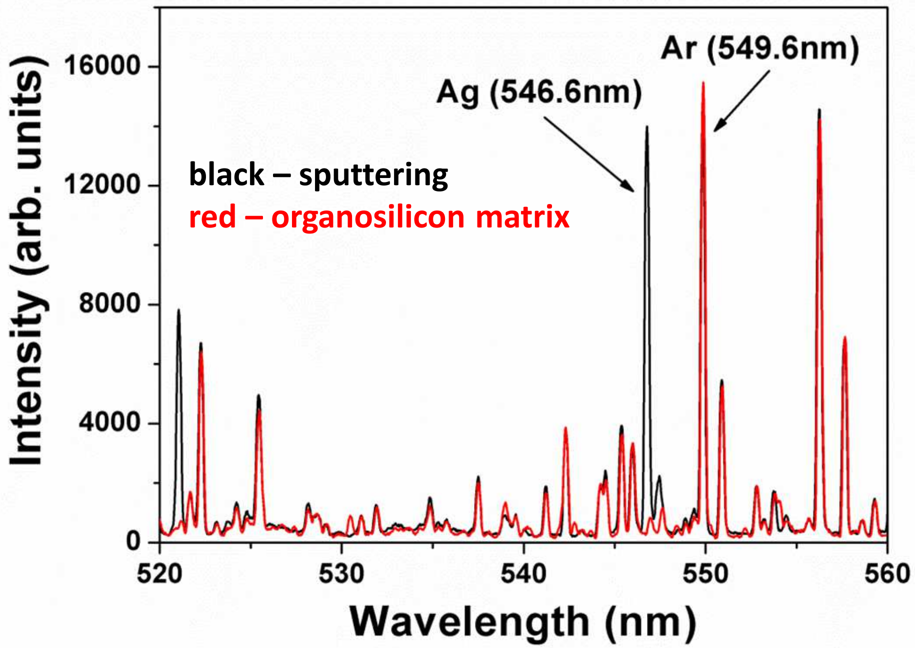

Scanning Electron Microscopy (SEM) images

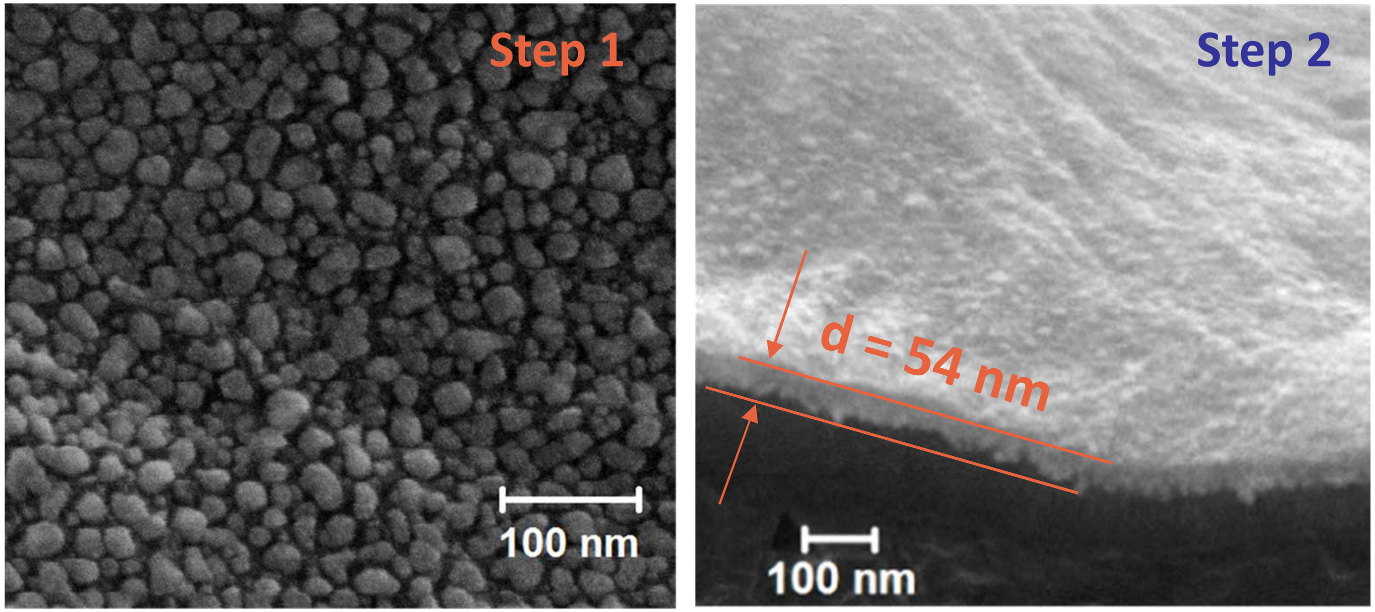

Isolated nanoparticles

AgNPs density:
1.7×10^{11} cm^{-2}

AgNPs mean size:
20.0 ± 10.0 nm

Left panel - SEM plane view image of the AgNPs layer deposited on LDPE substrate;
Right panel - SEM cross-section view image in Energy Dispersive X-ray Spectrometry (EDX) mode of the AgNPs/SiO_xC_y:H stack on LDPE substrate.

$$\Delta E = \frac{\rho_s}{\varepsilon}$$

$E = 1.2 \times 10^7$ V/m

Structural characterization

ATR-FTIR spectra

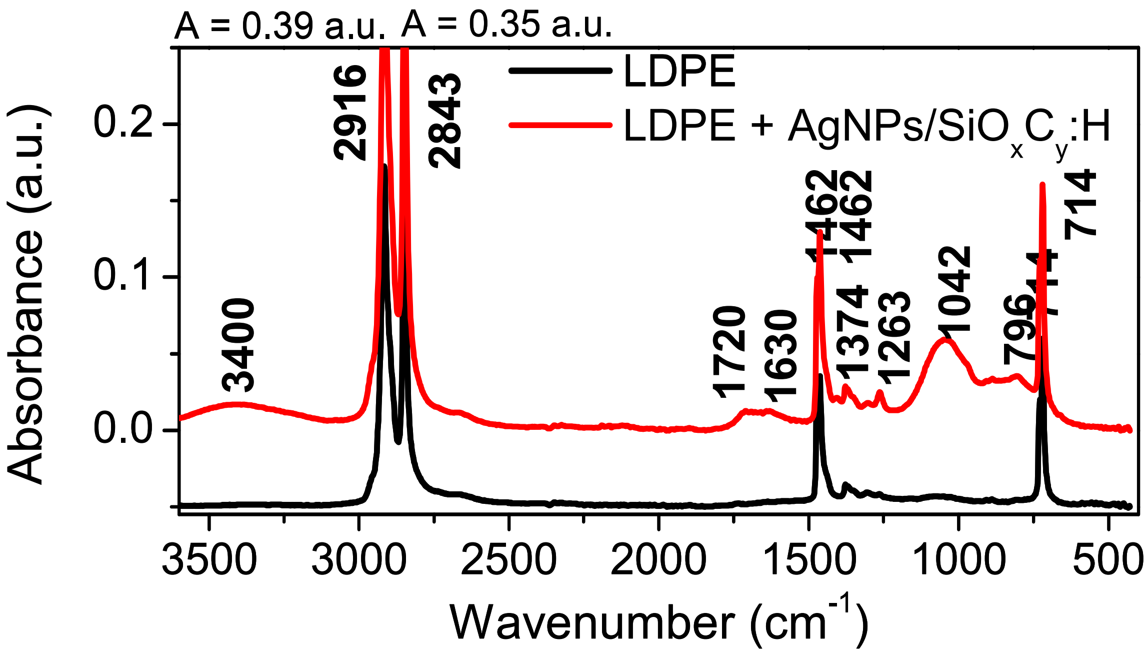

The bare LDPE sample and the tailored by AgNPs/SiOC:H stack one were characterized by Fourier Transform InfraRed spectroscopy in Attenuated Total Reflectance (ATR-FTIR) in the range 400 – 4000 cm^{-1}. The spectra were acquired with a Brucker Vertex 70 spectrometer to get information about the layer structure.

IR pick assignment

714 cm^{-1}	**$\gamma_r(CH_2)$**	**rocking**
810 cm^{-1}	**Si-O-Si**	**symmetrical stretching**
	Si-O-C	**(bending)**
1042 cm^{-1}	**Si-O-Si**	**asymmetrical stretching**
(1020 cm^{-1}	**Si-CH$_{x(x<2)}$-Si wagging mode)**	
1374 cm^{-1}	**$\delta(CH_3)$**	**bending**
1410 cm^{-1}	**C-H – in $SiCH_3$**	**rocking**
1462 cm^{-1}	**$\delta(CH_2)$**	**bending**
2843 cm^{-1}	**$\nu_g(CH_2)$**	**stretching**
2904 cm^{-1}	**C-H – in CH_3**	**asymmetrical stretching**
2916 cm^{-1}	**$\nu_a(CH_2)$**	**stretching**
3450 cm^{-1}	**OH – associated**	
3630 cm^{-1}	**OH – free**	

L. Milliere et al., (2016) J. Phys. D: Appl. Phys., **49**, 015304.

Pulsed Electro Acoustic (PEA) method

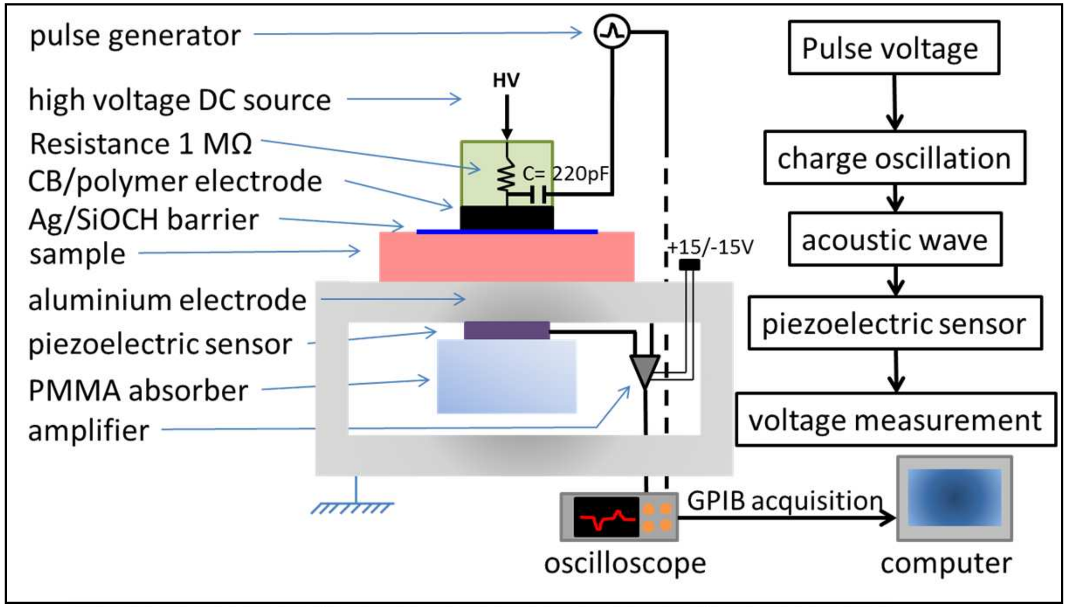

Acquisition of a space charge profile in 30 s steps (1kHz pulse generator, 600V amplitude)

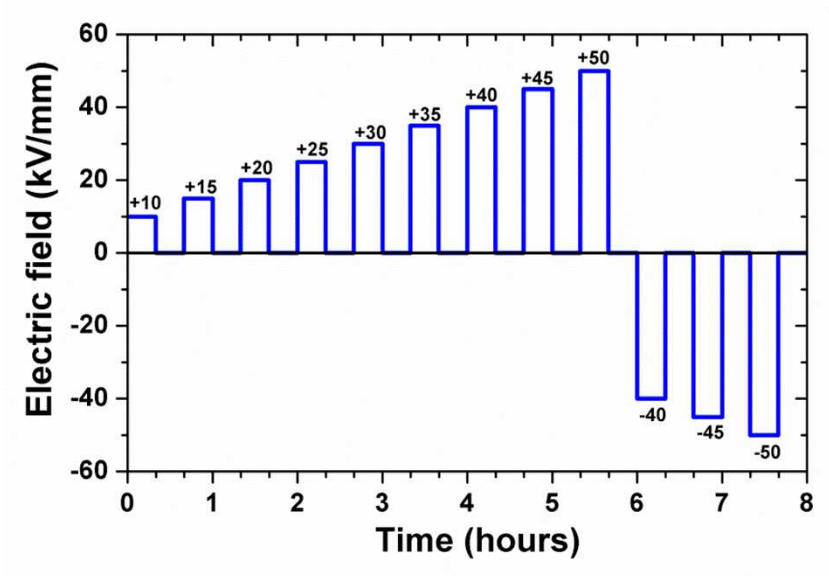

Field applied for 20 min with voltage rising rate being set to 1 kV/s;

Collaboration -> C. Laurent and G. Teyssedre, DSF group, LAPLACE

AgNPs as deep artificial traps of charges

Pulsed Electro Acoustic method

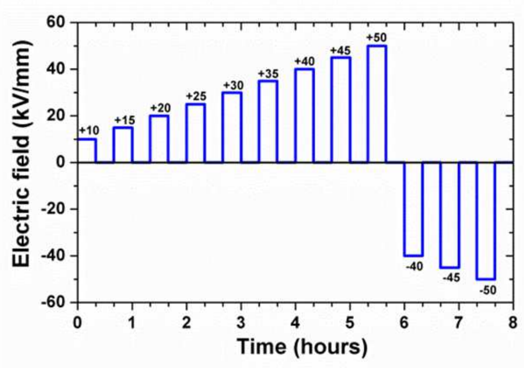

Reference LDPE – typical behavior with a space charge density below 10 C/m^3.

Tailored LDPE by an AgNPs/SiOC:H stack – absence of charge injection from the SC electrode.

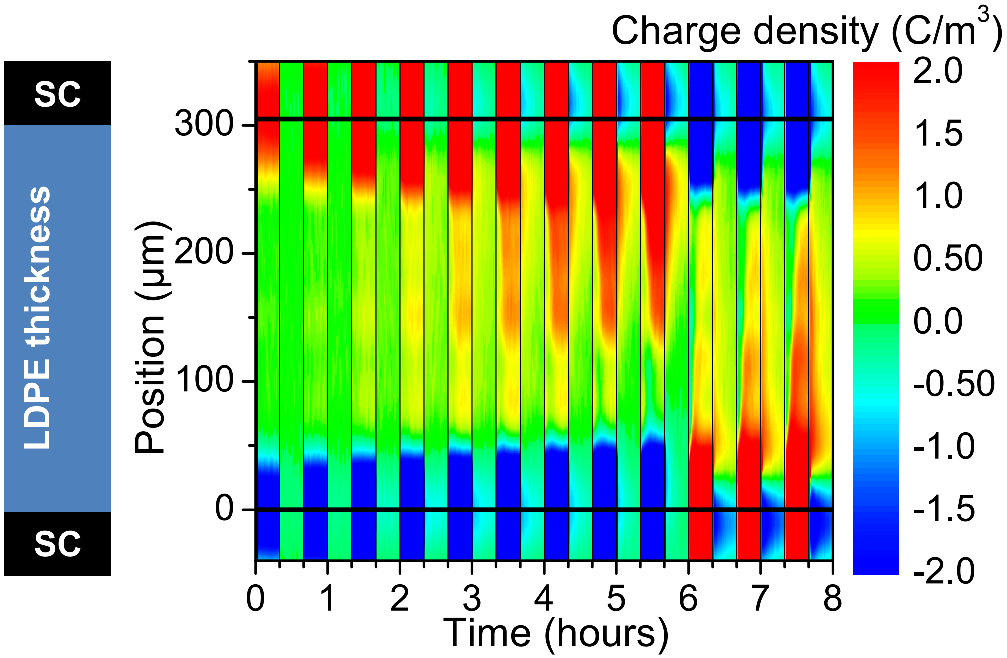

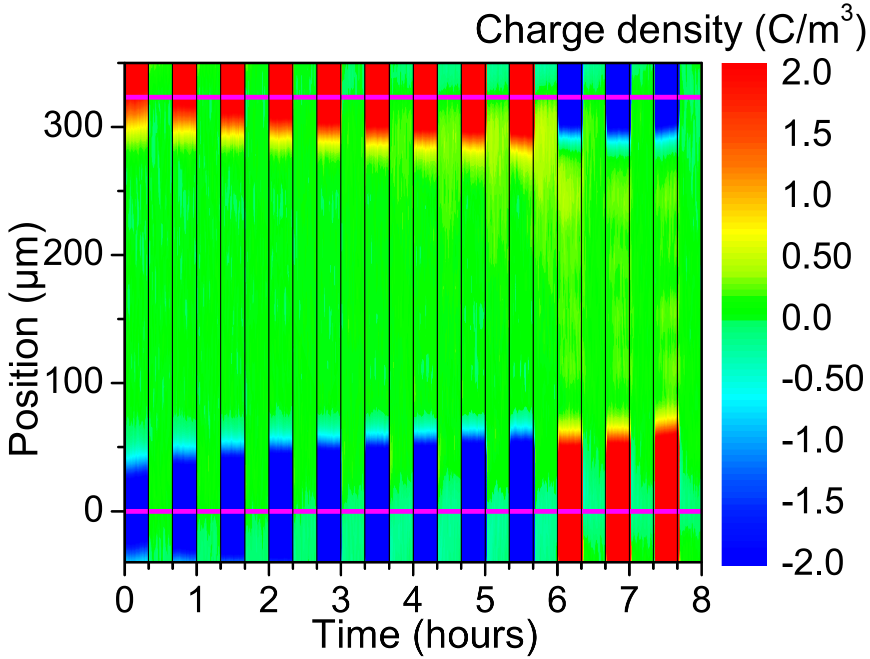

Field intensification of 5.8 kV/mm at the cathode and field decrease of 8.8 kV/mm at the anode at the end of the positive voltage step.

L. Milliere et al., (2016) J. Phys. D: Appl. Phys., **49**, 015304.

On a quantitative aspect – a field reduction at the electrode of about 1.2 × 10^7 V/m (with a Ag-NP density of 1.7 × 10^{11} cm^{-2} and a relative permittivity of 2.2 for LDPE).

AgNPs as deep artificial traps of charges

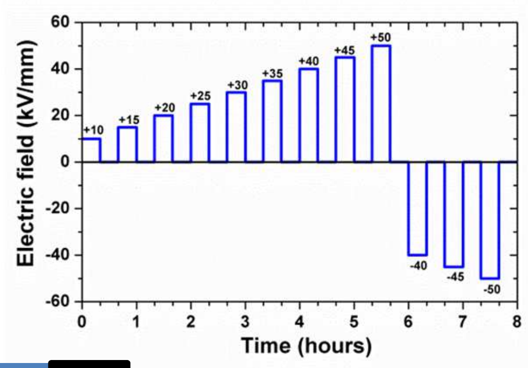

Pulsed Electro Acoustic method

Reference LDPE – typical behavior with a space charge density below 10 C/m³.

Tailored LDPE by an AgNPs/SiOC:H stack – absence of charge injection from the SC electrode.

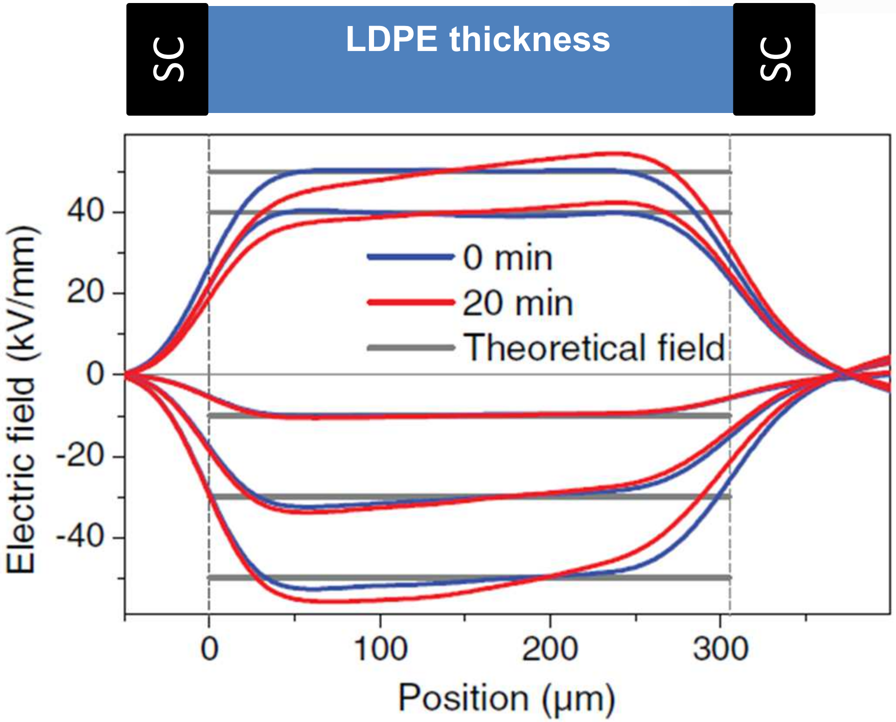

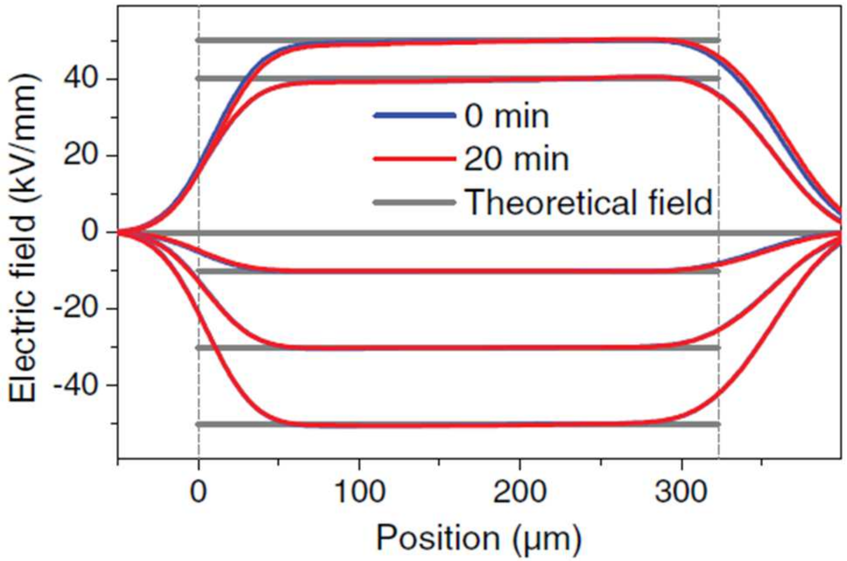

Field intensification of 5.8 kV/mm at the cathode and field decrease of 8.8 kV/mm at the anode at the end of the positive voltage step.

L. Milliere et al., (2016) J. Phys. D: Appl. Phys., **49**, 015304.

On a quantitative aspect – a field reduction at the electrode of about 1.2 × 10^7 V/m (with a Ag-NP density of 1.7 × 10^{11} cm^{-2} and a relative permittivity of 2.2 for LDPE).

AgNPs as deep artificial traps of charges -summary

- An efficient barrier effect in a LDPE sample tailored by a AgNPs/plasma polymer stack is achieved for applied fields well above the usual service fields for HVDC applications.
- A single layer of AgNPs embedded in an organosilicon matrix at a distance of few tens of nanometers from the SC/polyethylene contact suppresses the formation of bulk space charge following injection from the contact.
- The AgNPs introduce deep trapping centers for the injected charge thereby reducing the electric field at the contact and countering the injection process.
- Tailoring the surface of LDPE films with an AgNPs/SiO_xC_y:H stack provides a viable solution for space charge moderation. It also opens the way for understanding charging effects in nanocomposite materials.
- Owing to the versatility of the plasma process, as regards to the AgNPs size, density, and distance between the nanoparticles, the charging properties of polymeric materials can be tuned.

AgNPs based plasmonic substrates

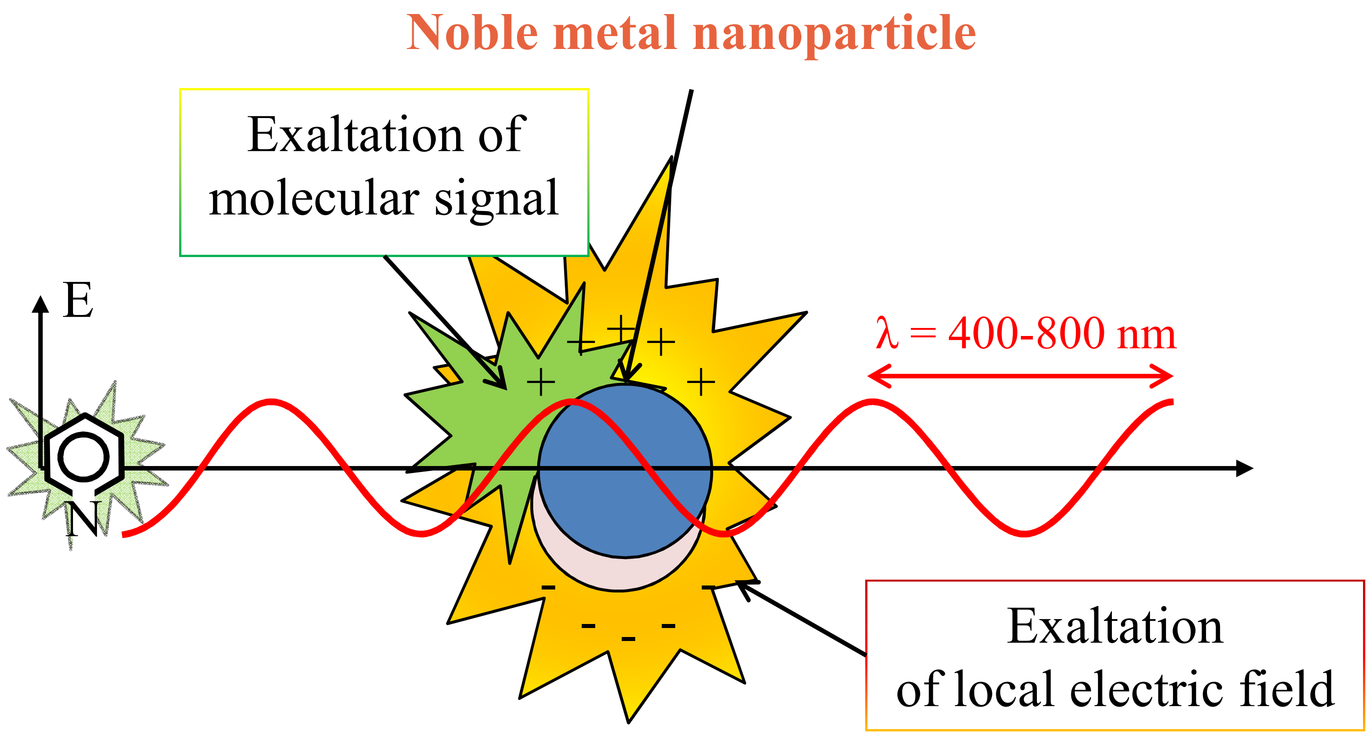

- Localized Surface Plasmons: electromagnetic field exaltation
- Antenna to enhance optical signal of nano-objects located in their vicinity
- **AgNPs are the best plasmonic antenna in the visible range**

AgNPs for biological surface effect

Biofilm is bacterial population adhered to a surface and enveloped by extracellular polymeric substances

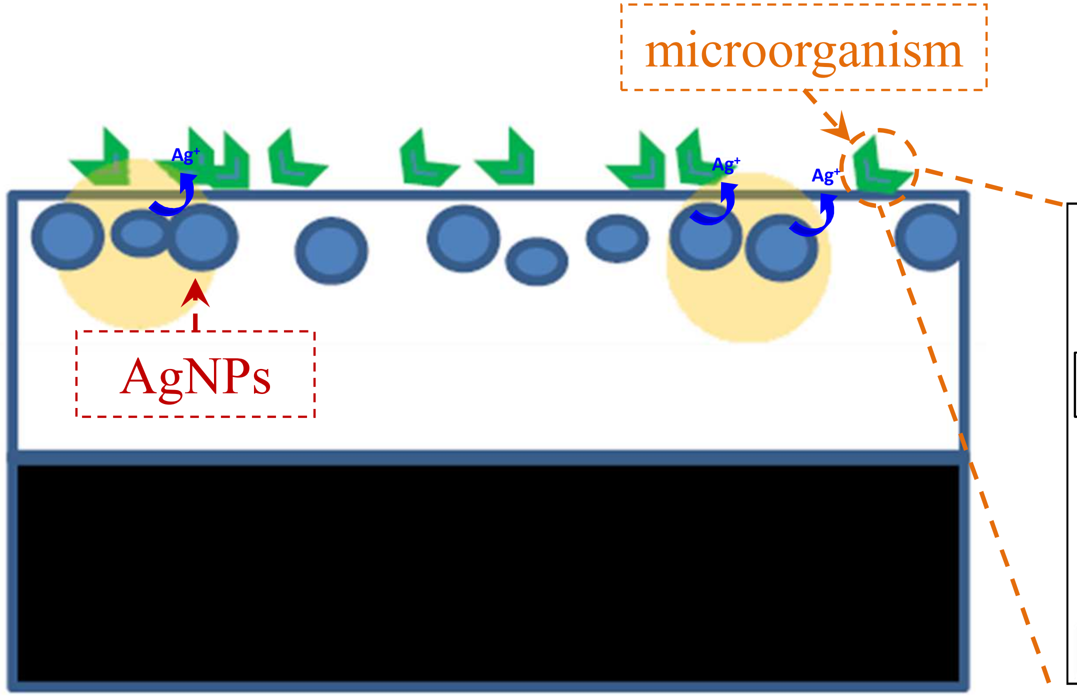

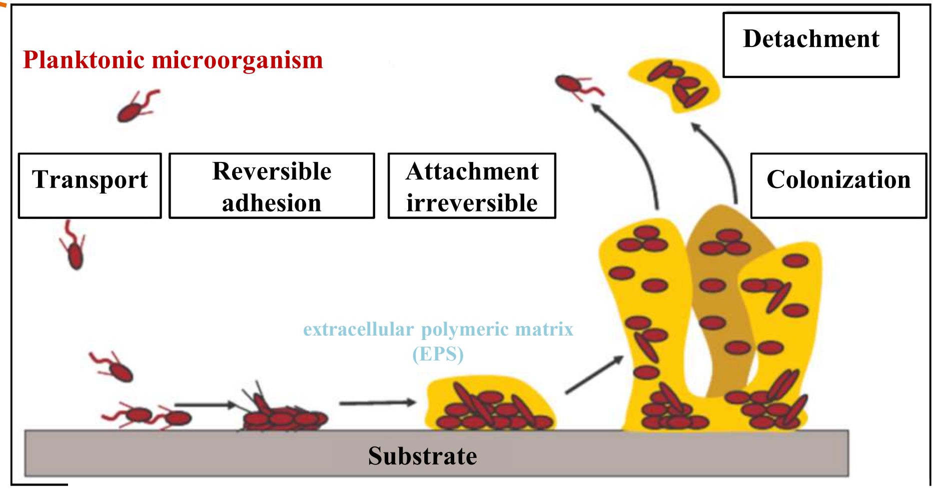

Filloux and Vallet, *Medecine/Sciences*, **19**, 77-83 (2008)

- Use the **multifunctionality** of AgNPs embedded in silica layers **(at the same time biocide agent and plasmonic antenna)** to **prevent biofilm** formation
- **Biocide effect** of AgNPs **goes through protein groups** of the cell

  => **study of this interaction at the nanometric scale**

C. Saulou et al., (2010) Anal. Bioanal Chem, **396**, 1441.

1-AgNPs as plasmonic antenna for spectroscopy and
2-AgNPs and/or Ag^+ as antibacterial agents

AgNPs for detection and prevention of biofilm formation

Power - P = 40 W and Time - t = 5 sec

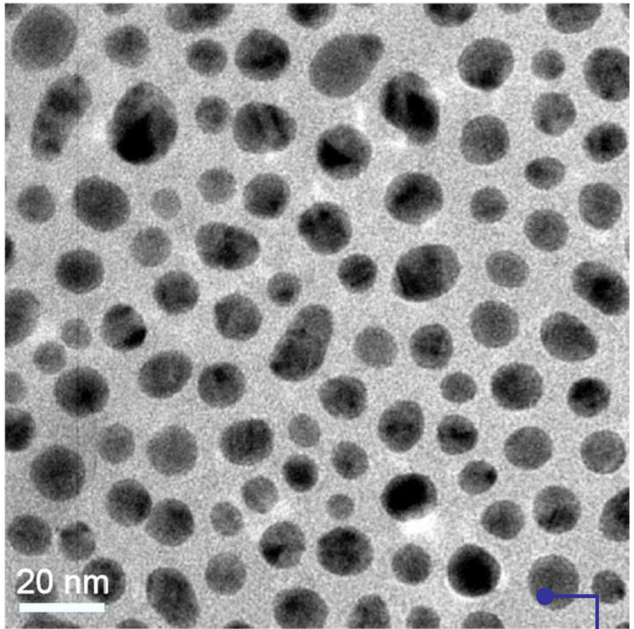

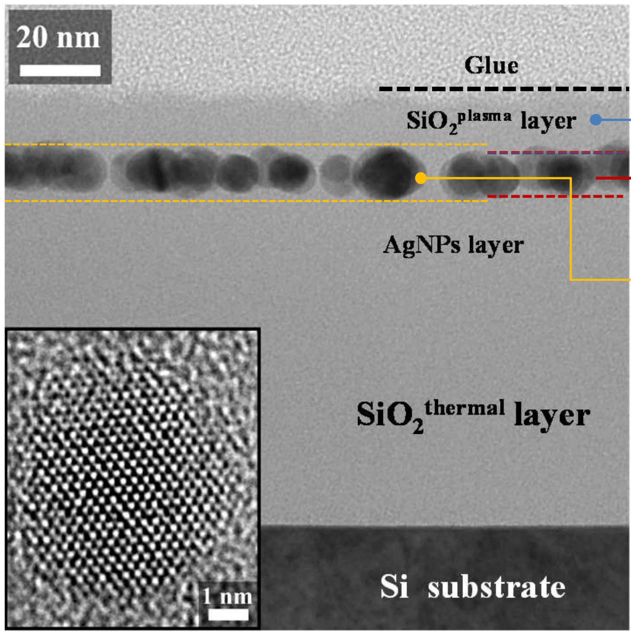

- Thickness $_{\text{layer plasma SiO}_2}$: 13.1 nm (roughness: 2.4 nm)
- <Thickness> $_{\text{layer Ag-NPs}}$: 8.9 nm
- Thickness $_{\text{layer Ag-NPs}}$ (MAX): 11.9 nm (for Molarity's calculus)

- <Ag-NPs diameter-like> $_{\text{Gauss fit}}$: 11.1 nm
- Standard Deviation $_{\text{Gauss fit}}$: 2.4 nm
- FWHM $_{\text{Gauss fit}}$: 5.7 nm
- Ag-NPs density: 4.6 x 10^{11} NPs/cm^2
- Area covered: 45.8 %
- Molarity $_{\text{layer AgNPs}}$: 24.7 molar

(mass = 3.92909 x 10^{-15} g and volume = 1.47582 x 10^{-18} dm^3 for 567 NPs, Silver Volume fraction = 25.4 %)

A. Pugliara et al., (2015) MRX, **2**, 065005.
A. Pugliara et al. (2016) STOTEN, **565**, 863.

Collaboration -> **C. Bonafos, A. Mlayah and R. Carles, CEMES, Toulouse**
C. Roques and M.-C. Monje, LGC, Toulouse and E. Navarro, IPE-CSIC, Zaragoza

AgNPs based plasmonic substrates

High sensitivity of the plasma elaborated plasmonic substrates

t_s = 5s

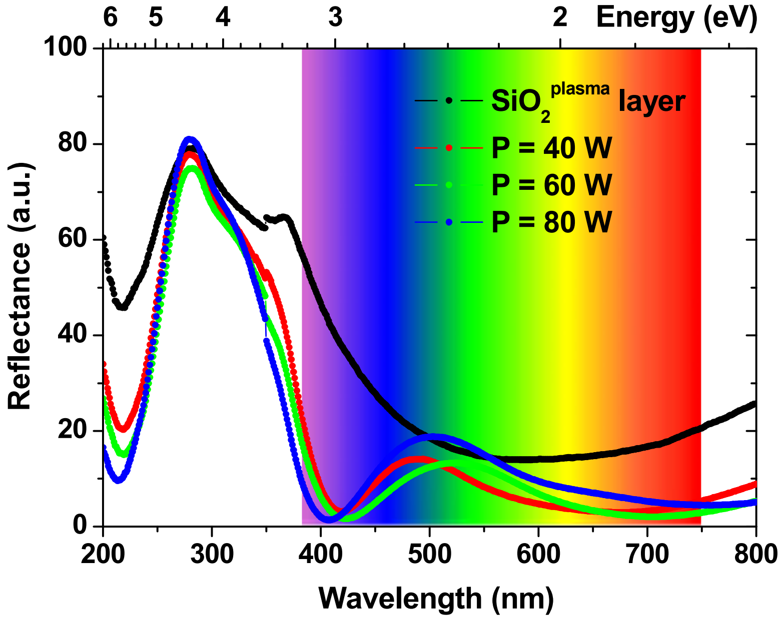

P = 10 W

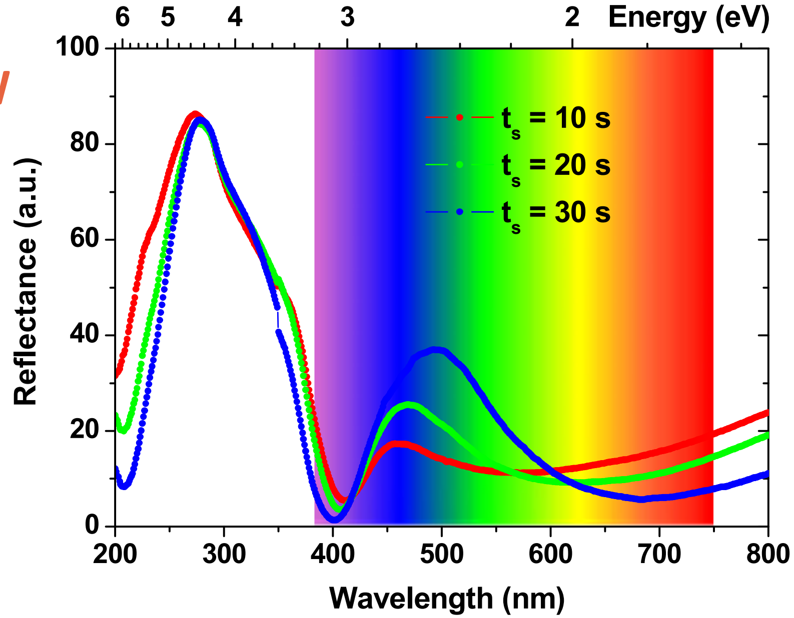

Power - P = 40 W; time - t_s = 5s;

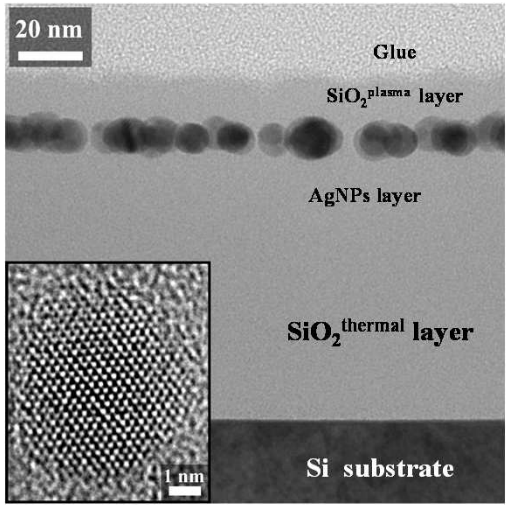

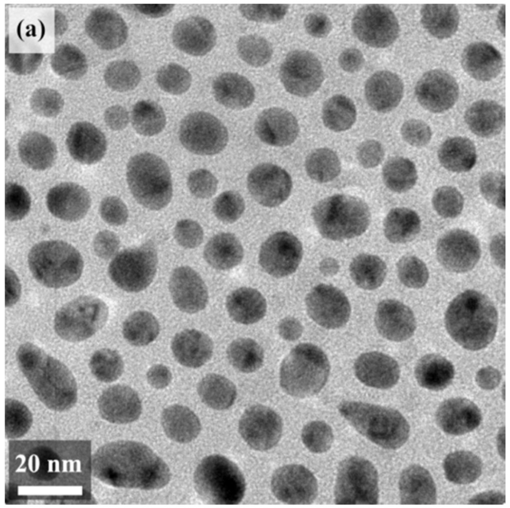

P = 80 W; t_s = 5s;

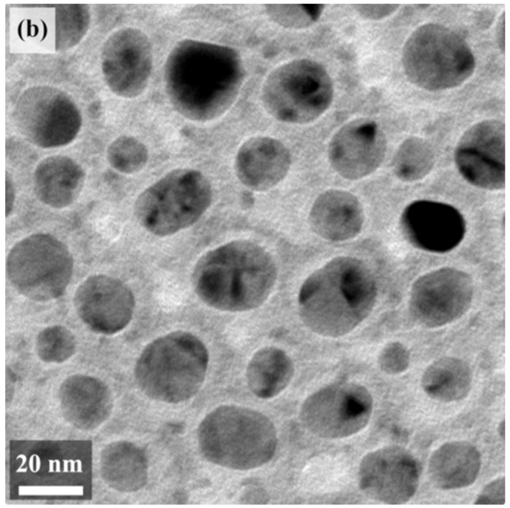

AgNPs for biological surface effects

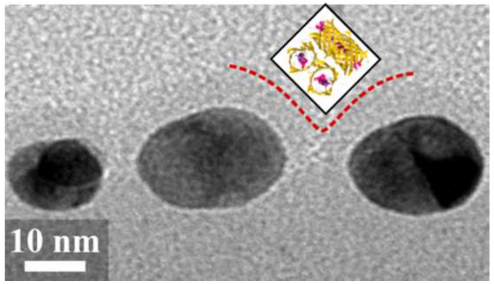

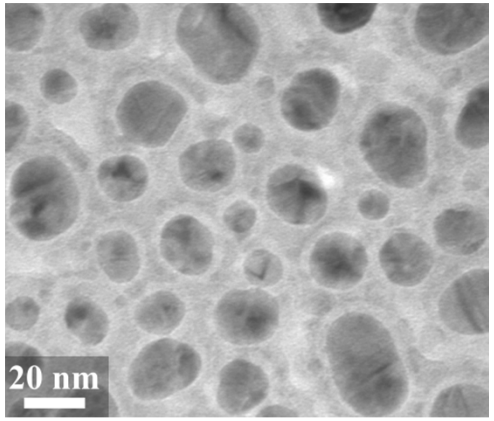

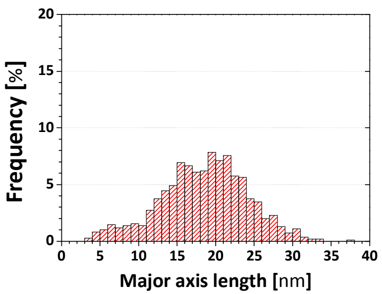

Surface Enhanced Raman Scattering (SERS) effect on DsRed protein layer deposited on the surface of plasmonic substrates.

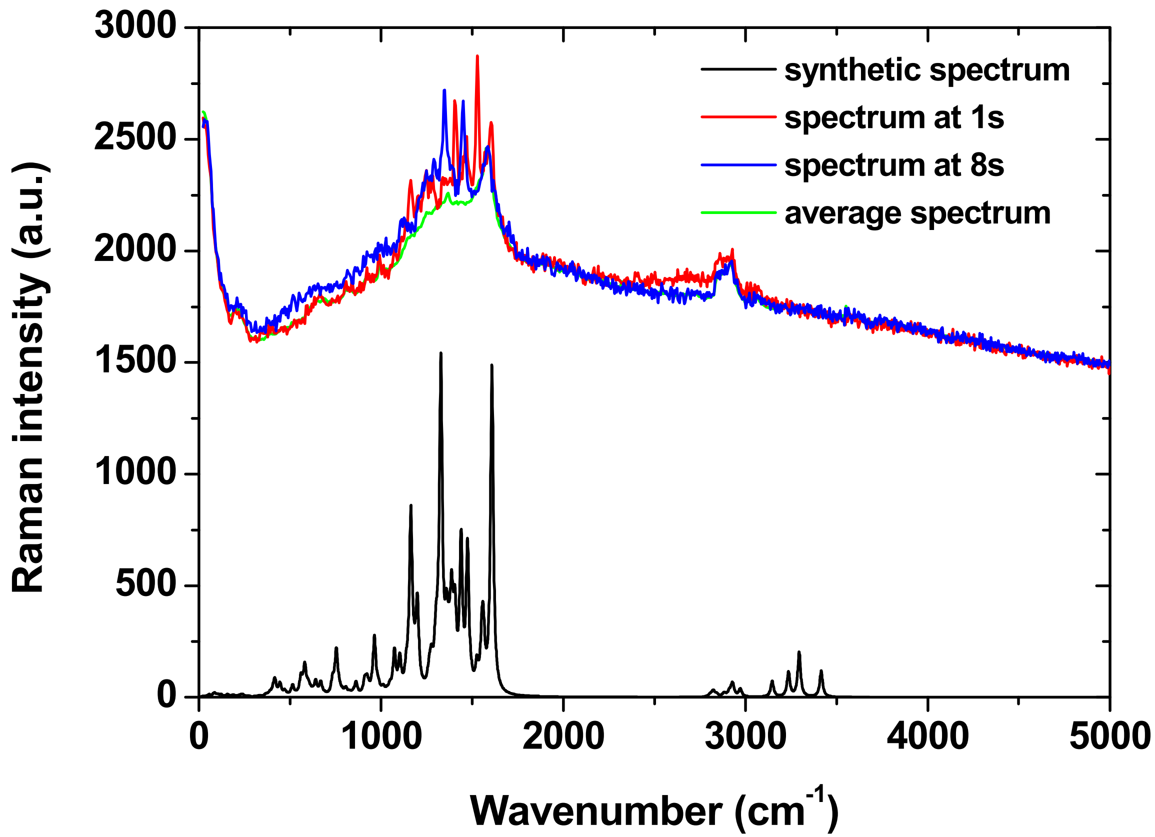

- **Development of the concept « spectro-inside » - using AgNPs as probes to detect optical signals from object closely located to the AgNPs**

M. Soumbo et al., (2016) IEEE Trans. NanoBioscience, **15**, 412.
M. Soumbo et al., (2016) IEEE NMDC Conf. Proceedings

Conclusion and perspectives

- The obtained characteristics of dehydrated DsRed droplet imply that the thickness of the adsorbed DsRed protein layer on solid SiO_2 surfaces can finely be tuned by the protein concentration.
- The DsRed proteins appear stable under pH-variations in line with previously reported studies.
- The adsorption of DsRed on SiO_2 surfaces and the following dehydration processes do not lead to protein denaturation.
- The photoluminescence emission of dehydrated DsRed proteins adsorbed on SiO_2 layers was found to peak at 590 nm, which is slightly red-shifted compared to the reported value for a solution.
- The FTIR spectrum confirms that the protein secondary structure is not destroyed after dehydration;
- Further studies will be oriented to studies of the interaction of DsRed proteins with silver nanoparticles (AgNPs) embedded in the silica layer at the surface vicinity.

Acknowledgments

Laurent Milliere, Alessandro Pugliara, Marvine Soumbo, Bernard Despax,
Gilbert Teyssedre, Christian Laurent, Christina Villeneuve-Faure, Laurent Boudou,
Laboratoire Plasma et Conversion d'Energie
Université de Toulouse, UPS, INPT, CNRS, LAPLACE, 118 route de Narbonne,
31062 Toulouse, France

Caroline Bonafos, Robert Carles, Adnen Mlayah
Centre d'Elaboration de Matériaux et d'Etudes Structurales
CEMES-CNRS, Université de Toulouse, 29 rue Jeanne Marvig, 31055 Toulouse, France

Christine Roques, Marie-Carmen Monje
Laboratoire de Génie Chimique
Université de Toulouse, UPS, INPT, CNRS, LGC, 4 allée Emile Monso, 31432 Toulouse, France

Stéphane Le Blond du Plouy
UMS 3623 - Centre de microcaractérisation Raimond Castaing
Université de Toulouse, 31000 Toulouse, France

Marie-Carmen Sancho and Enrique Navarro
Instituto Pirenaico de Ecología (CSIC)
Zaragoza, Spain

ANR project "InTail" ANR-AA-PBLI-II-2011

AAP-Programmes Recherche IDEX Transversalité 2013 project "ADAGIO" ANR-11-IDEX-0002-02

AAP-Programmes Recherche IDEX ATS 2015 project "SEPHIR" ANR-11-IDEX-0002-02